MEASUREMENT OF DRIVER/VEHICLE MULTILOOP RESPONSE PROPERTIES WITH A SINGLE DISTURBANCE INPUT

Duane T. McRuer, David H. Weir, Henry R. Jex,
Raymond E. Magdaleno, and R. Wade Allen*
Systems Technology, Inc., Hawthorne, California

ABSTRACT

Multiloop response properties of controllers are, in general, very difficult to obtain because an independent forcing function is needed for each describing function to be measured, and interpolation procedures may be required to obtain intermediate describing functions at common frequencies. Even then, a certain amount of untangling is required before the final results are obtained. When the loops which are closed and the nature of the describing function forms adopted in each loop are known or hypothesized, matters can be made much simpler. Then, the quantitative values of the individual describing functions can readily be identified using appropriate closed-loop describing function measures and decomposition procedures. Two examples are provided for the measurement of driver/vehicle multiloop response properties using a single disturbance input. The validity of the procedure is based on current multiloop operator adjustment rules and is made plausible by comparison with experimental data.

INTRODUCTION

The most common man/machine system in use today is a driver and an automobile, yet remarkably little is known empirically about the details of driver dynamic responses and how these interact with the vehicle dynamic characteristics. For instance, only one study of lateral control has been reported where driver describing functions were measured in an actual car (Ref. 1), and less than half a dozen studies have even been concerned with measurements in a simulator situation. A primary reason for this lack of attention resides in measurement difficulties due to the multiloop nature of most driver/vehicle system control situations of interest. The difficulties stem from the need for one independent input for each describing function to be measured, to the many couplings between the vehicle's state variables, to signal-to-noise problems, and last but not least, to data manipulation difficulties which include fairing and interpolation with already low confidence, dubious data and small differences between large uncertain numbers (Ref. 2). In spite of these difficulties, enough measurements now exist to support some key rules for multiloop human operations (Refs. 2-4). When these rules can be applied to specific situations, the fundamental difficulties can be bypassed and much simpler measurements can be made which nonetheless reflect the signficant multiloop human control characteristics (Refs. 5-6). In this paper these techniques are applied to the problem of driver steering control.

*President and Technical Director, Principal Research Engineer, Principal Research Engineer, Senior Research Engineer, and Senior Research Engineer, respectively.

VEHICLE AND DRIVER SUBSYSTEM DYNAMICS

The object of control in the driver/vehicle system is the automobile. Its dynamic characteristics for essentially constant speed steering maneuvers can adequately be described by equations of motion involving side velocity, v, heading rate, r, and roll angle, φ. The roll mode is least important in nominal maneuvers and many of the roll effects, such as roll steer and camber thrust, can be partially accounted for in the lateral velocity and heading degrees of freedom. Accordingly, the constant velocity lateral-directional characteristics can often adequately be approximated by the two-degree-of-freedom set:

$$\begin{bmatrix} s - Y_v & U_o - Y_r \\ -N_v & s - N_r \end{bmatrix} \begin{bmatrix} v \\ r \end{bmatrix} = \begin{bmatrix} Y_\delta \\ N_\delta \end{bmatrix} \delta \qquad (1)$$

Approximate values for the stability derivatives in terms of vehicle parameters and the key vehicle transfer functions for control inputs are summarized in the appendix. More complete automobile descriptions in six degrees of freedom are provided in Ref. 7.

Turn now to the driver. Driving tasks are often multiloop in nature. That is, the driver responds to more than one vehicle motion quantity. The key to multiloop driver models is the fundamental concept of manual vehicular control analysis: that the operator constructs feedback loops about the effective controlled element. The feedback quantities available to him for possible use consist of those:

- Directly sensed within the general visual field.
- Observable via visual displays.
- Directly sensed using modalities other than vision.

Quantities which can be perceived from the fixated visual field will show no scanning penalties, whereas those which require instrument scan or modification of the fixation point will introduce decrements in some driver dynamic features. For lateral steering control the feedbacks are derived from the general visual field and possibly supplemented by non-visual modalities. The feedback quantities actually selected by the driver will be those needed to satisfy the guidance and control needs and certain driver-centered requirements. The guidance and control needs are situation-specific. In the steering case, they involve an outer loop for lateral position control and an appropriate inner loop to provide damping for the low-frequency mode formed by virtue of closing the lateral position loop. These requirements are, of course, essentially independent of whether the controller is animate or inanimate.

The driver-centered requirements are central to the manual control, as opposed to the general control, problem. The human propensities and behavior associated with these requirements must be discovered by experiment. From the data available (Refs. 2-4), a series of adjustment rules similar to those for single-loop manual control systems can be stated. These include:

1. The feedback loops preferred are those which:
   a. Can be closed with minimum operator equalization.
   b. Require minimum scanning.
   c. Permit wide latitude in variation in the operator's characteristics.
2. Where distinct inner- and outer-loop closures can be defined by ordering the bandwidths (i.e., the higher the bandwidth, the more inner the loop), a series multiloop structure applies.
3. The adjustment of the variable gains in each of the loops is, in general, similar to that which would be used by a skilled automatic control designer who has available the same feedback entities. To a first approximation:
   a. The crossover model is directly applicable to many inner loop closures.

   b. The crossover model also holds for the outer loop with the proviso that the effective controlled-element transfer function includes the effects of all the inner-loop closures.
4. When scanning is not present, the remnant is primarily associated with the inner loop and is essentially the same as that for a single-loop system equivalent to the inner loop alone.

Other rules apply to situations where scanning is present; these are not pertinent here.

DRIVER/VEHICLE SYSTEM STRUCTURE

The combination of driver and vehicle into an appropriate control system for lateral position can conceivably be accomplished using a wide variety of feedback quantities. A number of these have been investigated theoretically in Refs. 8 and 9. One of the most likely possibilities when guidance and control requirements, driver-centered requirements, availability of cues in the visual field, and interpretation of such experimental evidence as driver eye movements are considered is an outer loop in lateral position, y, and an inner loop involving either path angle or heading angle. Additionally, path rate and heading rate are pertinent for higher-frequency control action. When all evidence is taken into account, a very likely structure for many driving tasks is that shown in Fig. 1. In equation form, the quasilinear model for the driver is:

$$\delta_s = Y_y(j\omega)Y_\psi(j\omega)y_e(j\omega) - Y_\psi(j\omega)\psi(j\omega) + Y_\psi(j\omega)n(j\omega) \qquad (2)$$

The describing function, Y_yY_ψ, characterizes the driver's operations on functions of the position error, whereas Y_ψ alone represents the driver's operations on functions of heading angle. The portion of the driver's output which is not linearly correlated with any disturbance or command inputs is modeled by the remnant, n.

It is important to note that the above presumed structure in no way implies direct perception of either lateral position or heading angle as such, but only that the driver responds in part to some function of these

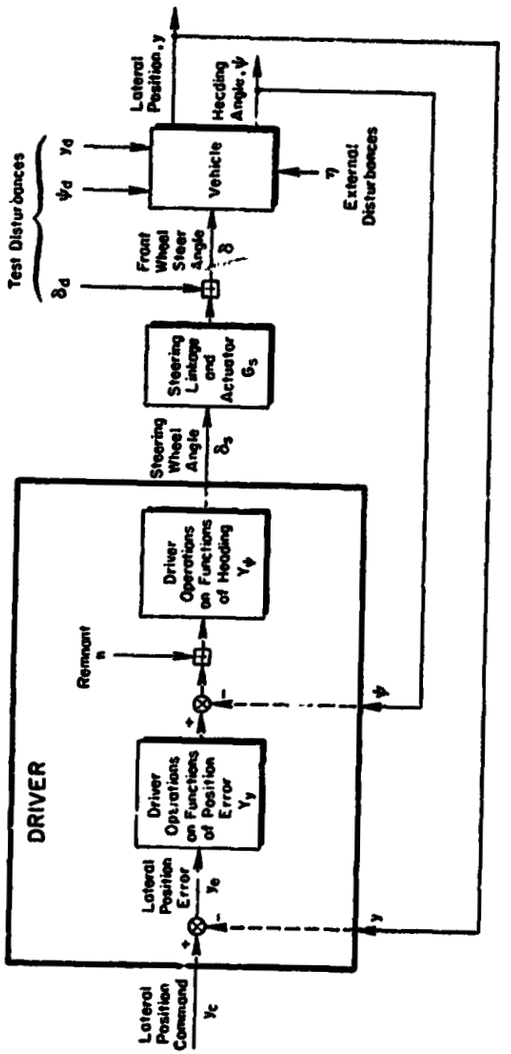

Figure 1 Block Diagram of Driver-Vehicle System for Lateral Steering Control

variables as sensed from the available visual field and non-visual modalities. In other words, although Eq. 2 is expressed explicitly in terms of lateral position and heading angle, any other possible feedbacks which are linear functions of y and ψ are also handled implicitly.

When y and ψ actually are the direct functions used by the driver in the experimental situation of interest, then in the light of the multiloop principles listed above heading should be an inner and lateral position an outer loop, and the low- and mid-frequency characteristics of Y_y should be a simple gain and those of Y_ψ a gain plus time delay. Since some vehicle dynamics present challenges which are readily overcome with heading rate, the higher-frequency portion of Y_ψ should include a lead. This can be considered as either high-frequency lead generation on ψ (with little or no degradation in effective time delay) or direct sensing of yawing velocity. The latter is pertinent for supra-threshold values of yawing velocity, r, as sensed by the vestibular system. Thus, the driver dynamics which we will ultimately use are given by:

$$Y_y = K_y$$
$$Y_\psi = K_\psi e^{-j\omega\tau}(T_L j\omega + 1) \qquad (3)$$

More extensive high-frequency characterization can be used with appropriate changes in τ. For example, when distinctions are to be drawn between different power steering systems, or when the effects of alcohol on the neuromuscular system are to be considered, a more extensive analytical description of the neuromuscular system can be added to Y_ψ with τ adjusted accordingly.

If interpretation of data obtained using these specific forms are in reasonable accord with analytical implications, then this would be strong indirect evidence that the driver used ψ and y feedbacks directly in accomplishing the particular driving task considered. If, on the other hand, Y_y or Y_ψ as deduced from the task-specific data are much more complex dynamic forms, then alternate feedbacks should be considered.

GENERAL SYSTEM EQUATIONS

In the study of driver/vehicle interaction in steering tasks, a number of system inputs require consideration. The most obvious are the lateral positional command, y_c, and external disturbances, η, because they are representative of actual roadway conditions. As shown in Fig. 1, y_c is actually present in the driver component of the closed-loop system, i.e., the lateral position command actually acting on the system is to some extent driver induced. The general character of the command is, however, determined by the roadway, lane pattern, obstacles to be avoided, etc. It can be as simple as a prescribed pathway with narrow tolerances and as complex as a tortuous way through freeway traffic. The external disturbances can arise from the atmosphere, such as yawing velocity, r_g, or side velocity, v_g, gusts, from roadway-induced disturbances, or from specially-contrived force and/or moment generators attached to the vehicle (e.g., a rocket). In addition to these inputs into the driver/vehicle system, various test disturbances are of interest for special measurement applications. The three most common are indicated in Fig. 1. The first, δ_d, is a front wheel steer angle applied in series with the driver's steering wheel input. The δ_d input is readily applied in actual or simulated cars by the addition of an extensible link or other differential device into the steering system. The heading and path disturbances, ψ_d and y_d, are primarily of values in simulator applications, where these signals are readily added within the equations of motion. These test disturbances enter the equations of motion at the locations shown in Fig. 2. They can, for example, be readily applied to the servo drive of a television camera used to generate the visual scene from a model landscape, as in Refs. 10 and 11 .

The equations of motion for lateral position and heading with these forcing functions and disturbances and using Y_y and Y_ψ for generality are given by:

$$\begin{bmatrix} (1+Y_yY_\psi G_s G_\delta^y) & Y_\psi G_s G_\delta^y \\ Y_yY_\psi G_s G_\delta^\psi & (1+Y_\psi G_s G_\delta^\psi) \end{bmatrix} \begin{bmatrix} y \\ \psi \end{bmatrix} = \begin{bmatrix} 1 & U_o/s & G_\delta^y & Y_yY_\psi G_s G_\delta^y & Y_\psi G_s G_\delta^y & G_\eta^y \\ 0 & 1 & G_\delta^\psi & Y_yY_\psi G_s G_\delta^\psi & Y_\psi G_s G_\delta^\psi & G_\eta^\psi \end{bmatrix} \begin{bmatrix} y_d \\ \psi_d \\ \delta_d \\ y_c \\ n \\ \eta \end{bmatrix}$$

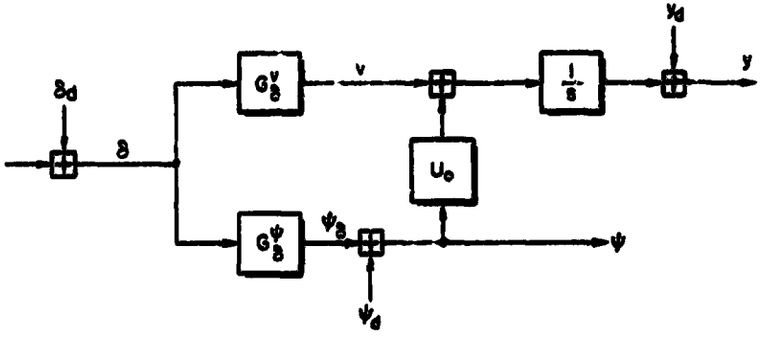

Figure 2. Test Disturbance Entry Locations in Vehicle Dynamics

The front wheel steer angle is provided by the auxiliary equation:

$$\delta = \delta_d + Y_yY_\psi G_s(y_c \quad y) + Y_\psi G_s(n - \psi) \qquad (5)$$

The closed-loop system responses of heading, lateral position, and front wheel steer angle are given as functions of the forcing function and disturbances in Table 1. The multiloop character of this system is indicated by the sum of $Y_\psi G_s G_\delta^\psi$ and $Y_yY_\psi G_s G_\delta^y$ in the denominator and the presence of the coupling numerator terms, $G_{\eta\delta}^{y\psi}$ and $G_{\eta\delta}^{\psi y}$, shown in the ψ and y numerator expressions (Ref. 12). The two primes on the denominator indicate that two loops are closed.

Closed-loop describing function measurements can be made using any of the forcing functions or disturbances, or combinations of these which are independent. Because the remnant acts as a continuous power spectral density, it will tend to contaminate any such measurements as a noise. However, if input power is large w compared with the remnant when both are reflected to a point of interest in the system, this contamination will be negligible. In any event, it can generally s assessed directly by consideration of the

TABLE 1

CLOSED-LOOP SYSTEM DYNAMICS

Denominator:

$$D'' = 1 + Y_\psi G_s (G_\delta^\psi + Y_y G_\delta^y) = 1 + Y_\psi G_s G_\delta^y \left[1 + \frac{U_o Y_y}{s} + \frac{Y_{\dot{y}}}{s} G_\delta^{\dot{y}}\right]$$

y Numerator:

$$D''y = Y_y Y_\psi G_s G_\delta^y y_c + (1 + Y_\psi G_s G_\delta^\psi) y_d + Y_\psi G_s G_\delta^y n + G_\delta^y \delta_d + (G_\eta^y + Y_\psi G_s G_{\eta\delta}^{y\psi})\eta + \left(\frac{U_o}{s} - Y_\psi G_s \frac{G_\delta^{\dot{y}}}{s}\right)\psi_d$$

ψ Numerator:

$$D''\psi = Y_y Y_\psi G_s G_\delta^\psi y_c - Y_y Y_\psi G_s G_\delta^\psi y_d + Y_\psi G_s G_\delta^\psi n + G_\delta^\psi \delta_d + (G_\eta^\psi + Y_y Y_\psi G_s G_{\eta\delta}^{\psi y})\eta + \left(1 + Y_y Y_\psi G_s \frac{G_\delta^{\dot{y}}}{s}\right)\psi_d$$

δ Numerator:

$$D''\delta = Y_y Y_\psi G_s y_c - Y_y Y_\psi G_s y_d + Y_\psi G_s n + \delta_d - Y_\psi G_s (Y_y G_\eta^{\dot{y}} + G_\eta^\psi)\eta - Y_\psi G_s \left(1 + \frac{U_o Y_y}{s}\right)\psi_d$$

relative power at the frequencies involved. One of the tricks in multiloop measurement is to select a family of describing functions which indicate high signal-to-noise ratios over particular (different) frequency ranges.

The fundamental measurement problem is to determine Y_y, Y_ψ, and remnant power spectral densities, Φ_{nn}. In principle, to obtain Y_y and Y_ψ separately, two independent inputs will be required. As noted already, the early work on multiloop human operator measurements had to use several independent inputs because the general nature of quantities such as Y_y and Y_ψ were to be discovered. Now that we have some appreciation for at least the likely form of these quantities, as given in Eq. 3, a simpler procedure can be used with only one input. The inputs to be considered should satisfy two fundamental criteria:

- The closed-loop describing functions should have a large frequency range over which signal to noise is high, i.e., remnant power should be small compared to forcing function or disturbance power at common points with the system.
- The closed-loop describing functions should be differentially sensitive to Y_y and Y_ψ in different frequency bands so that the properties of Y_y and Y_ψ can be readily untangled.

For these reasons, the principal disturbances and forcing functions that have been used are y_c, δ_d, ψ_d, and y_d. The first two are applicable to both actual vehicles on the road and simulator operations, whereas the latter two are suitable only in a simulator. Measurements with a disturbance, while having great value in peculiar situations, tend to be extraordinarily muddled because of the coupling features introduced via the coupling numerators. It is better to stay with inputs acting directly within one of the loops rather than a disturbance which is diffused into both loops via complex vehicular couplings.

Two particular examples will be illustrated in more detail below. These are describing functions measured with a steering or with a heading disturbance as the test input.

TYPICAL DESCRIBING FUNCTIONS WITH STEERING DISTURBANCES

The front wheel steer angle response with a steering disturbance as the system forcing characteristic and remnant is given by specialization of Table 1, i.e.:

$$\delta = \frac{1}{1 + Y_\psi G_s\left(G_\delta^\psi + Y_y G_\delta^y\right)}\left[\delta_d + Y_\psi G_s n\right] \tag{6}$$

At frequencies where remnant effects can be considered negligible, an effective open-loop system can be formed by considering δ_d as the input and δ the error. Then the quantity $\delta_d/\delta - 1$ parallels the quantity $(I/E) - 1$, which is equivalent to the open-loop transfer function in a single-loop system. Performing this operation gives:

$$\begin{aligned}
\frac{\delta_d}{\delta} - 1 &= Y_\psi G_s\left(G_\delta^{\dot\psi} + Y_y G_\delta^y\right) \\
&= Y_\psi G_s\left[G_\delta^\psi\left(1 + \frac{U_o Y_y}{s}\right) + \frac{Y_y}{s} G_\delta^y\right] \\
&= Y_\psi\left[1 + \frac{U_o Y_y}{s} + \frac{Y_y}{s}\frac{G_\delta^y}{G_\delta^\psi}\right] G_s G_\delta^\psi \\
&= Y_p^* G_s G_\delta^\psi
\end{aligned} \tag{7}$$

where

$$\begin{aligned}
Y_p^* &= Y_\psi\left[1 + \frac{U_o Y_y}{s} + \frac{Y_y}{s}\frac{G_\delta^y}{G_\delta^\psi}\right] \\
&= Y_\psi\left[1 + Y_y \frac{G_\delta^y}{G_\delta^\psi}\right]
\end{aligned} \tag{8}$$

Here the quantity Y_p^* is seen to be obtained by taking the closed-loop response measurement, δ/δ_d, inverting it, subtracting 1, dividing out the known transfer function of the steering linkage and vehicle, $G_s G_\delta^\psi$. Y_p^* is particularly simple in form in that the driver's heading describing function, Y_ψ, is a multiplicative factor, while Y_y enters into the bracketed expression in a relatively simple way.

At this point, let us examine the properties of the bracketed expressions in Eq. 8. In terms of the lateral equations of the automobile, this is given by:

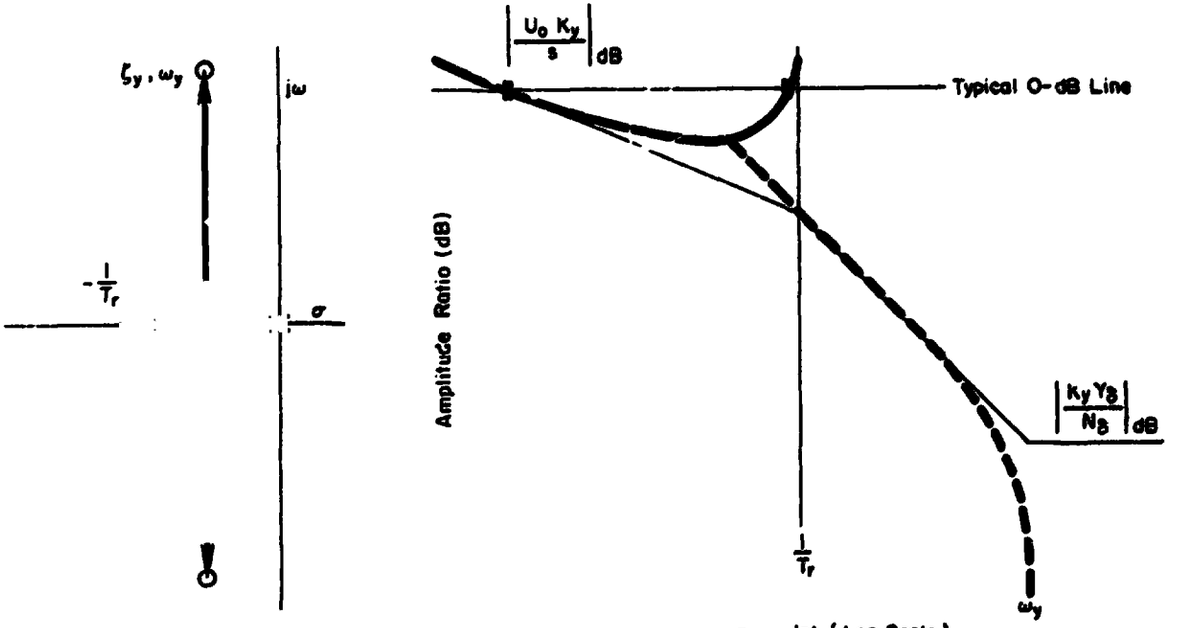

a) Conventional Root Locus

b) Bode Root Locus

Figure 3. System Survey of Roots of $1 + K_y(G^Y_\delta/G^\psi_\delta)$

$$1 + Y_y \left\{ \begin{matrix} G_\delta^y \\ G_\delta^\psi \end{matrix} \right\} = 1 + Y_y \left\{ \begin{matrix} Y_\delta \\ N_\delta \end{matrix} \frac{\left[s^2 + 2(\zeta\omega)_y s + \omega_y^2 \right]}{s(s + 1/T_r)} \right\} \tag{9}$$

Using the relationships developed in the appendix for the two-degrees of freedom equations this becomes:

$$1 + Y_y \left\{ \begin{matrix} G_\delta^y \\ G_\delta^\psi \end{matrix} \right\} = 1 + Y_y \left\{ \frac{a}{k_z^2} \frac{\left[s^2 + \left(\frac{1}{T_r} \right) s + \frac{aU_o}{k_z^2} \left(\frac{1}{T_r} \right) \right]}{s\left(s + \frac{1}{T_r} \right)} \right\} \tag{10}$$

The roots of Eq. 9 can be readily evaluated if it is viewed as the result of a loop-closing operation in which the transfer function, $Y_y\{\ \}$, is the open-loop transfer function. At this point, we bring to bear the multiloop operator adjustment rules previously described and substitute for the general outer-loop driver describing function, Y_y, the much more specific form, K_y. A system survey which shows the roots of $1 + K_y\{\ \}$ is given in Fig. 3. The Bode root locus there indicates the closed-loop roots as the driver gain, K_y, is varied. The conventional root locus, which shows the same effects, is remarkable in that it is an example from practice of an academic anomaly, i.e., the damping of the quadratic zeros is approximately the same as the heading transfer function numerator inverse time constant, $1/T_r$. This approximation is exact for the two-degree-of-freedom lateral-directional equations when the z axis radius of gyration, k_z, is equal to the geometric mean between the car dimensions, a and b.

The path loop is the outer loop, so typically the gain, K_y, is relatively low. Then, a nominal zero dB line on the Bode root locus would be as shown in Fig. 3. The σ-Bode (locus of all real roots) is essentially on the low-frequency asymptote at this point; consequently, one of the roots will be given almost exactly by:

$$\sigma_1 = -U_o K_y \tag{11}$$

Because of the peculiar approximate relationship between $2(\zeta\omega)_y$ and $1/T_r$, the sum of the closed-loop roots is constant in spite of the variation in

gain (this is not, of course, true for a general open-loop system with a quadratic numerator and denominator). Under these special circumstances, the second root will be given by:

$$\begin{aligned} \sigma_2 &= -(1/T_r - U_o K_y) \\ &= -1/T_r' \end{aligned} \tag{12}$$

With these literal approximate factors, the value of $1 + K_y(G_\delta^y/G_\delta^\psi)$ becomes:

$$1 + K_y \frac{G_\delta^y}{G_\delta^\psi} \doteq \frac{U_o K_y \left(\frac{j\omega}{U_o K_y} + 1 \right) \left(T_r' j\omega + 1 \right)}{j\omega(T_r j\omega + 1)} \tag{13}$$

When the form for Y_ψ provided by the multiloop adjustment rules is used in conjunction with Eq. 13, the total describing function, Y_p^o, is seen to have the form:

$$Y_p^o \doteq \frac{U_o K_y K_\psi \left(T_L j\omega + 1 \right) \left(\frac{j\omega}{U_o K_y} + 1 \right) \left(T_r' j\omega + 1 \right) e^{-j\omega\tau}}{j\omega(T_r j\omega + 1)} \tag{14}$$

An asymptotic Bode plot of this is shown in Fig. 4. Here, it will be noted that the low-frequency asymptote defines the outer-loop gain uniquely, while the mid-frequency horizontal asymptote is just the gain, K_ψ. The breakpoint between the very low-frequency and mid-frequency asymptotes is $U_o K_y$. The high-frequency breakpoint gives the indication of any inner-loop lead. Actual data are presented on Fig. 5. They show the same characteristic concave-upward basket-like shape of the sketch of Fig. 4. Quick approximations to the values of K_y, K_ψ, and $1/T_L$ are readily obtained by fairing in the asymptotic plot. By keeping in mind the shape and functional relations involved in the asymptotes, comparative describing function data and parameters can be directly assessed by eyeball.

Precise values for the driver characteristics are most easily determined with an optimal curve-fitting routine. The routine adjusts the Y_p^o parameters

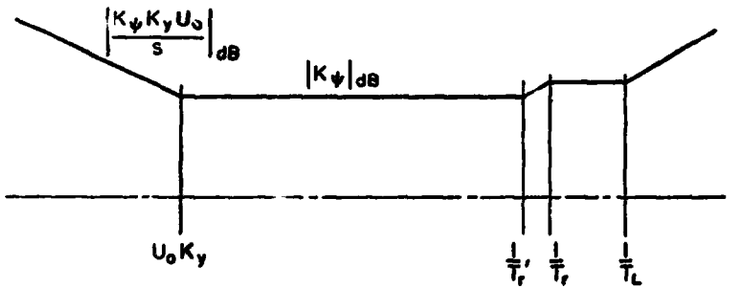

Figure 4. Asymptotic Bode Plot for $|Y_p^*|$

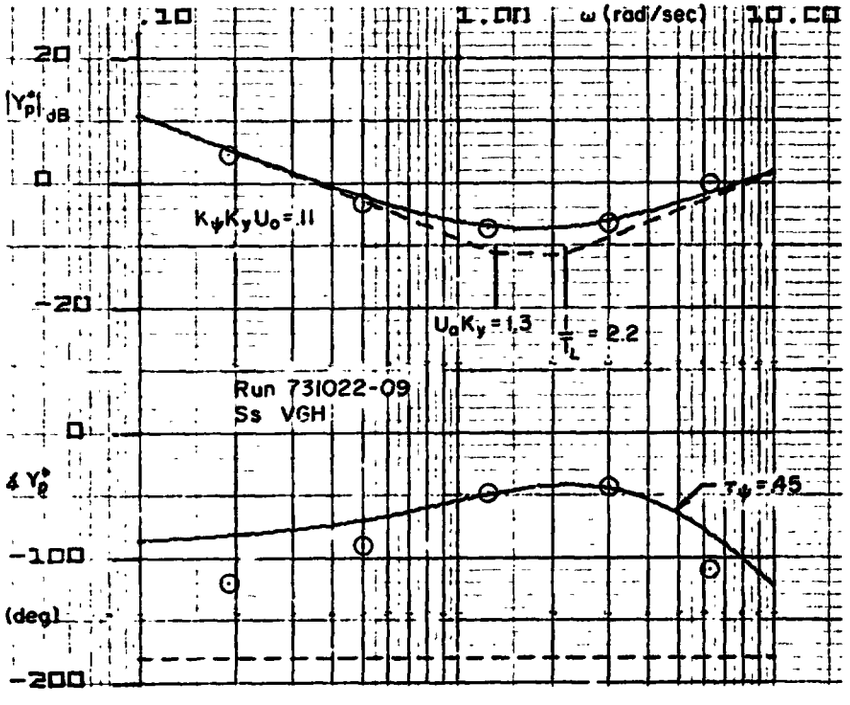

Figure 5. Example Y_p^* Data and Curve Fit

including the effective time delay, τ, to simultaneously fit amplitude and phase. An example curve fit is also shown on Fig. 5 (although the T_r, T_r' dipole in Eq. 14 was not included for simplicity).

As a practical matter, the measurements are quite simple to obtain with sums of sinusoids and on-line describing function measurements. These are then inexpensively reduced and curve-fitted on a routine basis. Thus, the previously highly-complex multiloop reduction procedures are reduced to an elementary and inexpensive set of operations. The shape of the data further confirms the multiloop describing rules presented earlier, in that the data behave according to the predictions.

Y_p^* data can be interpreted in alternate ways which are helpful when considering actual perceptual structures which the driver may be using. For example, excellent single-loop driver/vehicle systems result when the driver is assumed to act on the "time-advanced lateral deviation," $y(t+T)$, or the "aim-point-heading" error, ψ_L. Both are shown in Fig. 6 and both involve an aim point at a distance, R, down the road. With the first:

$$y(t+T) \doteq y + U_o \gamma T = (Ts + 1)y \qquad (15)$$

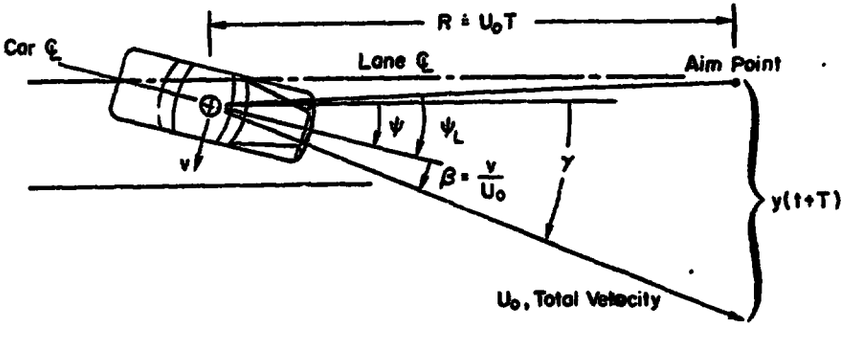

Figure 6. Motion Quantities for Directional Control

In this interpretation, the low-frequency lead breakpoint in Fig. 4 is just $1/T$. Thus:

$$1/T = U_o K_y \doteq U_o/R \tag{16}$$

Note that:

$$K_y \doteq 1/R \tag{17}$$

the inverse of the aim point distance down the road. With ψ_L, the aim point heading error:

$$\psi_L \doteq \psi + y/R \tag{18}$$

If the composite feedback quantity, $Y_\psi(\psi + K_y y)$, in Eq. 2 is identified with ψ_L, then K_y is simply $1/R$, just as above. With either of these variables as the basis for control, there is an *effectively single-loop* closure, with the kinematic relation $1/R$ corresponding to K_y, and $1/U_o K_y$ or R/U_o to the low-frequency lead time constant.

MULTILOOP DESCRIBING FUNCTIONS WITH HEADING DISTURBANCE

The closed-loop heading-to-heading-disturbance transfer function as obtained from Table 1 is:

$$\frac{\psi}{\psi_d} = \frac{1 + Y_y Y_\psi G_s \frac{1}{s} G_\delta^y}{1 + Y_\psi G_s \left[G_\delta^\psi \left(1 + \frac{U_o Y_y}{s} \right) + \frac{Y_y}{s} G_\delta^y \right]} \tag{19}$$

When this is considered in a fashion similar to that above, i.e., when ψ_d is taken as an input and ψ as the error of an equivalent single-loop feedback system, then the effective inner-loop describing function, $(\psi_d/\psi) - 1$, becomes:

$$\frac{\psi_d}{\psi} - 1 = Y_\psi G_s G_\delta^\psi \left[\frac{1 + \frac{U_o Y_y}{s}}{1 + Y_y Y_\psi G_s \frac{G_\delta^y}{s}} \right]$$

$$= Y_\psi G_s [G_\delta^\psi]' \tag{20}$$

where

$$[G_\delta^\psi]' = G_\delta^\psi \left[\frac{1 + \frac{U_o Y_y}{s}}{1 + Y_y Y_\psi G_s \frac{G_\delta^y}{s}} \right]$$

Here, the effective vehicle transfer function, $[G_\delta^\psi]'$, is the transfer function for the vehicle as seen by the heading loop as an outer loop, i.e., it reflects the lateral position loop closure. If, now, we insert the appropriate forms for vehicle and driver multiloop characteristics, Eq. 20 becomes:

$$\frac{\psi_d}{\psi} - 1 = \frac{U_o K_y K_\psi \left(\frac{j\omega}{U_o K_y} + 1 \right) \left(T_L j\omega + 1 \right) e^{-j\omega\tau_\psi}}{j\omega} \left[\frac{G_\delta^\psi(j\omega)}{1 + \frac{K_y K_\psi (T_L j\omega + 1) e^{-j\omega\tau_\psi} G_\delta^y(j\omega)}{j\omega}} \right] \tag{21}$$

An asymptotic Bode plot of this function is shown in Fig. 7. Here again the path loop dominates the low-frequency characteristics, while the heading inner loop is more significant at higher frequencies. In Fig. 7 note that the pole at very low-frequencies is non-minimum phase; hence, the phase curve starts at -270 deg. This pole arises from the terms in brackets in Eq. 21. This function can be used directly to fit data, as with the steering input considered previously. Typical data from Ref. 11, as well as some unpublished data from that series of experiments, is shown in Fig. 8. These data indicate a value of $U_o K_y$ of about 0.37 rad/sec whereby the low-frequency lead time constant is about 2.8 sec and, for a speed of 88 ft/sec (60 mph), the "aim point distance" would be about 240 ft.

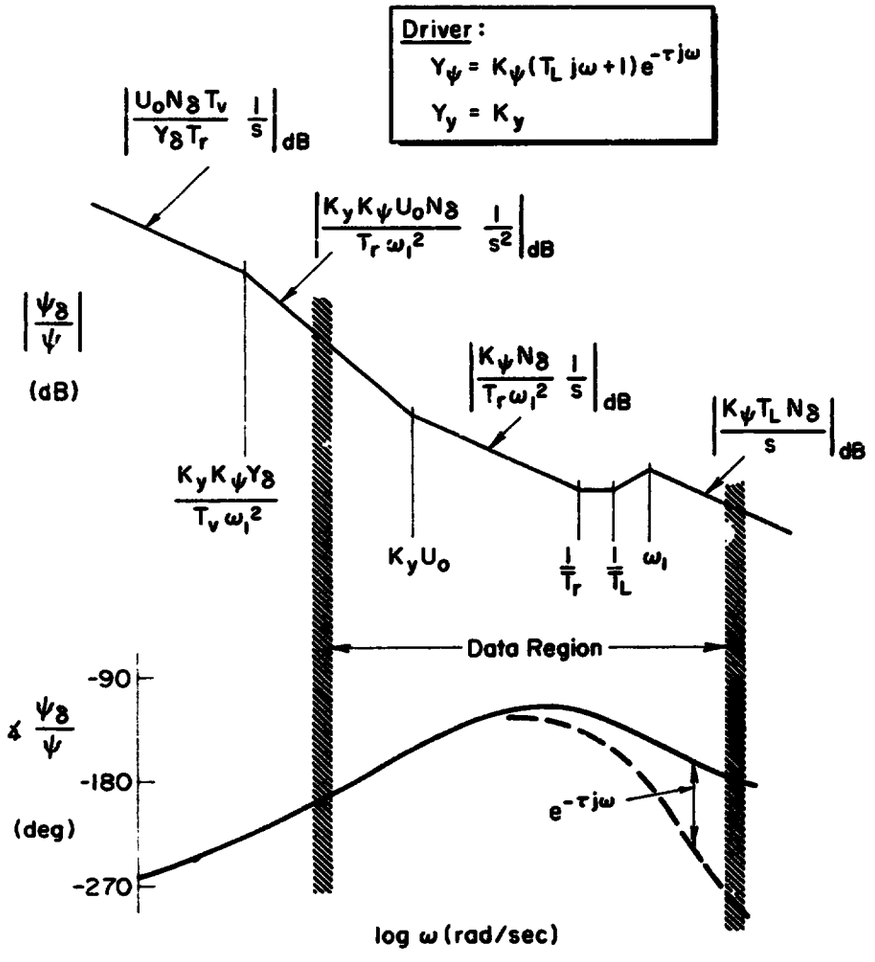

Figure 7. Open-Loop Driver/Vehicle Describing Function for Heading

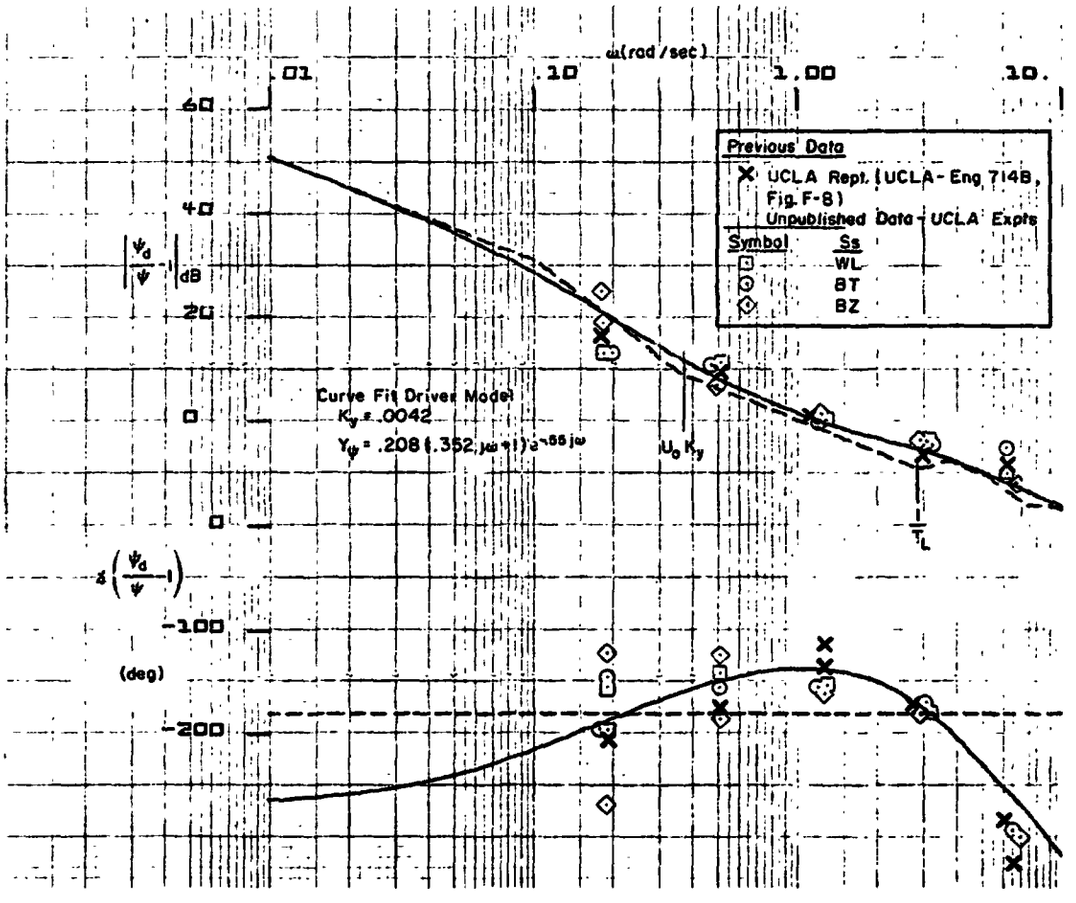

Figure 8. Effective Inner-Loop Describing Function Data and Curve Fit

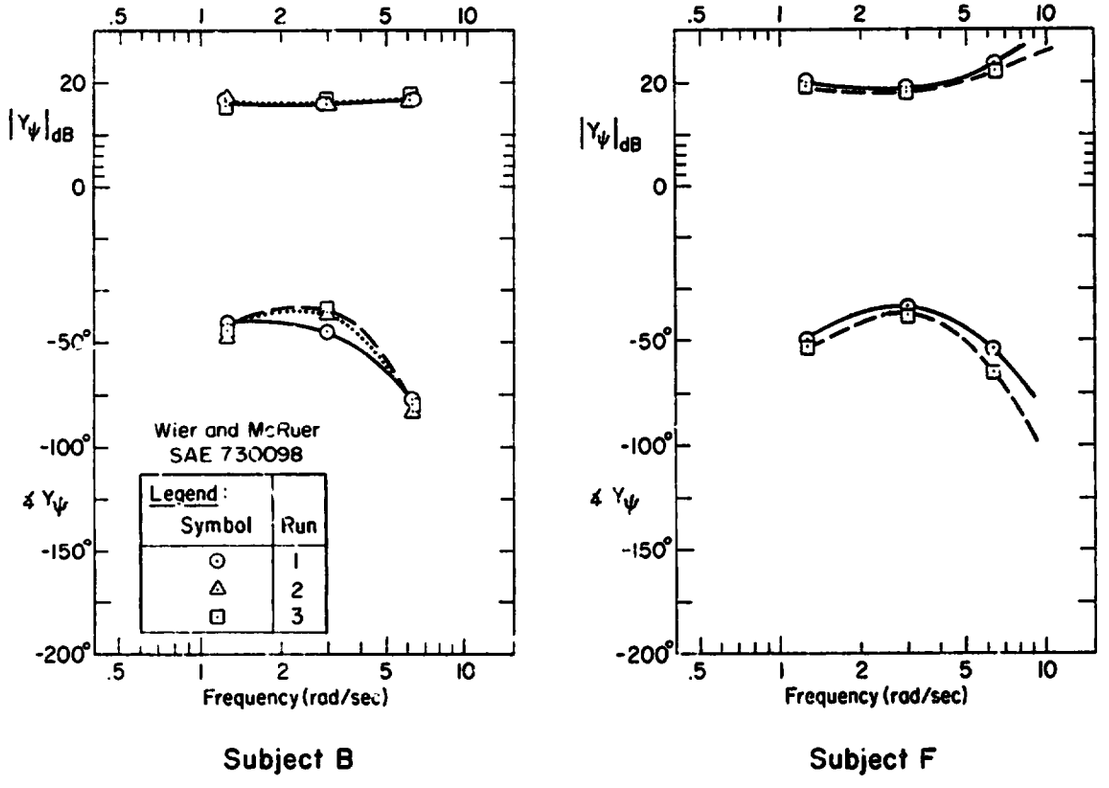

Figure 7. Interpreted Driver Alone Describing Functions for Inner Loop, Y_ψ (Ref. 13)

At upper middle to high frequencies, the effective vehicle transfer function, $[G_\delta^{\psi'}]$, is hardly affected by the path closure. Thus, at these frequencies:

$$[G_\delta^{\psi'}] \triangleq G_\delta^{\psi}$$

and

$$\frac{\psi_a}{\psi} - 1 \triangleq Y_y G_s G_\delta^{\psi} \qquad \text{at higher frequencies} \tag{22}$$

The driver's heading response describing function, Y_ψ, can then be isolated from the equivalent open-loop system high-frequency properties by removing the known vehicle and steering subsystem dynamic characteristics, $G_s G_\delta^{\psi}$. Typical data, from Ref. 13, are shown in Fig. 9. These demonstrate clearly the difference between Subject B and Subject F in that only the latter uses high-frequency lead generation. Again, the fact that data, such as shown in Figs. 8 and 9, tend to follow the trends predicted using the multiloop adjustment rules provides further verification.

Finally, an interesting comparison of the features of describing functions obtained from heading vs. steering disturbances can be seen in the low-frequency regions of Figs. 9 and 8. The Y_p^* steering disturbance case has K_y effects changing the low-frequency amplitude while the phase is insensitive (starting at −90 deg for any value of K_y). Just the opposite occurs for the heading disturbance case in Fig. 8 where the amplitude is relatively insensitive, while the phase curve moves directly with K_y.

CONCLUSIONS

The point of view taken in this paper permits the simple and routine estimation of the more significant driver characteristics in steering control tasks. The fundamental difficulties of multiloop measurements are avoided by tailoring the driver loop structure per the currently understood multiloop human operator adjustment rules. The simplifications so obtained permit multiloop car/driver situations to be analyzed as easily as systems which are essentially single loop and single input.

NOMENCLATURE

a	Distance of mass center aft of the front axle
b	Distance of mass center forward of the rear axle
G_s	Steering linkage transfer function
G_δ^v	Vehicle transfer function between steer angle and lateral velocity
G_δ^ψ	Vehicle transfer function between steer angle and heading angle
I_{zz}	Vehicle yaw moment of inertia
k_z	Vehicle radius of gyration, $\sqrt{I_{zz}/m}$
K_y	Driver gain for lateral position control
K_ψ	Driver gain for heading control
m	Vehicle mass
n	Driver remnant
r	Yawing velocity (heading angle rate)
s	Laplace transform complex variable
U_o	Nominal forward velocity
v	Side velocity
y	Lateral position of mass center (relative to an inertial frame)
y_c	Lateral position command to driver
y_d	Lateral position disturbance
Y_y	Driver describing function for lateral position control
Y_{α_1}	Side force due to front tire slip angle
Y_{α_2}	Side force due to rear tire slip angle
Y_ψ	Driver describing function for heading angle control
γ	Path angle
δ	Front wheel steer angle

δ_d Steer angle disturbance

δ_s Driver steering wheel angle

η General external disturbance

τ_e Effective time delay

ψ Heading angle

ψ_d Heading angle disturbance input

ω Frequency

REFERENCES

1. Delp, P., E. R. F. W. Crossman, and H. Szostak, "Estimation of Automobile-Driver Describing Functions From Highway Tests Using the Double Steering Wheel," Seventh Annual Conf. on Manual Control, USC, 2-4 June, 1971, NASA SP-281, pp. 223-236.

2. Stapleford, R. L., S. J. Craig, and J. A. Tennant, Measurement of Pilot Describing Functions in Single-Controller Multiloop Tasks, NASA CR-1278, Jan. 1969

3. Stapleford, R. L., D. T. McRuer, and R. Magdaleno, Pilot Describing Function Measurements in a Multiloop Task, NASA CR-542, Aug. 1966.

4. Weir, D. H., and D. T. McRuer, Pilot Dynamics for Instrument Approach Tasks: Full Panel Multiloop and Flight Director Operations, NASA CR-2019, May 1972.

5. Teper, G. L., "An Effective Technique for Extracting Pilot Model Parameter Values From Multi-Feedback, Single-Input Tracking Tasks," Eighth Annual Conf. on Manual Control, U. of Mich., 17-19 May 1972, pp. 23-34.

6. Teper, G. L., An Assessment of the "Paper Pilot" — An Analytical Approach to the Specification and Evaluation of Flying Qualities, AFFDL-TR-71-174, June 1972.

7. Weir, D. H., C. P. Shortwell, and W. A. Johnson, Dynamics of the Automobile Related to Driver Control, SAE Paper 680194, Feb. 1967.

8. Weir, D. H., and D. T. McRuer, "A Theory for Driver Steering Control of Motor Vehicles," Highway Res. Record No. 247, 1968, pp. 7-28.

9. Weir, D. H., and D. T. McRuer, "Dynamics of Driver/Vehicle Steering Control," Automatica, Vol. 6, No. 1, 1970, pp. 87-98.

10. Weir, D. H., and C. K. Wojcik, "Simulator Studies of the Driver's Dynamic Response in Steering Control Tasks," Driving Simulation, Highway Res. Record No. 364, 1971, pp. 1-15.

11. Wojcik, C. K., and R. W. Allen, Studies of the Driver as a Control Element, Phase 3, UCLA-ENG-7148, July 1971.

12. McRuer, D., D. Graham, and I. Ashkenas, Aircraft Dynamics and Automatic Control, Princeton Univ. Press (forthcoming).

13. Weir, D. H., and D. T. McRuer, Measurement and Interpretation of Driver Steering Behavior and Performance, SAE Paper No. 750098, Jan. 1975.

APPENDIX

LATERAL-DIRECTIONAL VEHICLE DYNAMICS

The two-degree-of-freedom lateral-directional equations for a car are given in Eq. 1. The stability derivatives are defined in terms of vehicle and tire design parameters by the expressions below.

$$Y_v = \frac{-2}{mU_o}(Y_{\alpha_1} + Y_{\alpha_2})$$

$$N_v = \frac{2}{I_{zz}U_o}(bY_{\alpha_2} - aY_{\alpha_1})$$

$$Y_r = \frac{2}{mU_o}(bY_{\alpha_2} - aY_{\alpha_1})$$

$$N_r = \frac{-2}{I_{zz}U_o}(a^2Y_{\alpha_1} + b^2Y_{\alpha_2})$$

$$Y_\delta = \frac{2}{m}Y_{\alpha_1}$$

$$N_\delta = \frac{2a}{I_{zz}}Y_{\alpha_1}$$

The transfer functions of interest are:

Heading Angle:

$$\frac{\psi}{\delta} = G_\delta^\psi = \frac{1}{s} G_\delta^r = \frac{N_\delta (s + 1/T_r)}{s[s^2 + 2\zeta_1\omega_1 s + \omega_1^2]}$$

Side Velocity:

$$\frac{v}{\delta} = G_\delta^v = \frac{Y_\delta (s + 1/T_v)}{[s^2 + 2\zeta_1\omega_1 s + \omega_1^2]}$$

Lateral Position:

$$\frac{y}{\delta} = G_\delta^y = \frac{Y_\delta [s^2 + 2\ell_{y,y} s + \omega_y^2]}{s^2[s^2 + 2\zeta_1\omega_1 s + \omega_1^2]}$$

where

$$2\zeta_1\omega_1 = -(Y_v + N_r) \quad ; \quad \omega_1^2 = N_v(U_o - Y_r) + Y_v N_r$$

$$1/T_r = -Y_v + \frac{Y_\delta}{N_\delta} N_v \quad ; \quad 1/T_v = -N_r - \frac{N_\delta}{Y_\delta}(U_o - Y_r)$$

$$2\ell_{y,y} = -N_r + \frac{N_\delta}{Y_\delta} Y_r \quad ; \quad \omega_y^2 = \frac{U_o N_\delta}{Y_\delta}\left(-Y_v + \frac{Y_\delta}{N_\delta} N_v\right) = \frac{U_o N_\delta}{Y_\delta}\left(\frac{1}{T_r}\right)$$

In terms of the vehicle parameters:

$$\frac{1}{T_r} = \frac{2}{mU_o}\left(\frac{a + b}{a}\right) Y_{\alpha_r}$$

$$2\ell_{y,y} = \frac{2b}{I_{zz} U_o}(a + b) Y_{\alpha_r} = \frac{mab}{I_{zz}}\left(\frac{1}{T_r}\right) = \frac{ab}{k_z^2}\left(\frac{1}{T_r}\right)$$

If the radius of gyration in yaw, k_z, is the geometric mean of the c.g. to axle dimensions, a and b, then $2\ell_{y,y}$ will be equal to $1/T_r$.

ABSTRACT

AN EXPERIMENTAL STUDY OF THE MOTORCYCLE ROLL STABILIZATION TASK

David J. Eaton

The stabilization task of the motorcycle rider has been studied experimentally, using data from actual road tests. In each experiment, the test subject, whose upper body was restrained by a rigid brace, controlled the motorcycle roll angle by applying a steering torque to the handlebars. Roll angle, roll rate, steering torque, and steering angle were recorded for three test subjects. Experiments were restricted to the steady-state, straight path, constant forward speed (usually 30 mph) situation.

The strongest source of excitation to the man-motorcycle system was found to be the rider's remnant. To minimize bias errors in identifying a linear transfer function representing the rider, a technique developed by Wingrove and Edwards of the NASA Ames Research Center was employed. The results are consistent with a theoretical analysis of the man-motorcycle system, using classical automatic control theory.